

Structure and Phonons of the Ice Surface

J. Braun, A. Glebov, A. P. Graham, A. Menzel, and J. P. Toennies

Max Planck Institut für Strömungsforschung, Bunsenstr. 10, D-37073 Göttingen, Germany

(Received 6 October 1997)

The structure and phonon dynamics of the ice surface, prepared by growing thick ice layers (~ 100 Å) on Pt(111), were investigated using high resolution helium atom scattering. Ice layers grown at $T_s = 125$ K were found to be well ordered, with a complete bilayer (1×1) surface termination, as shown by diffraction measurements at $T_s = 30$ K. Time-of-flight spectra provide evidence for an intense longitudinal shearing mode, large multiphonon background, and enhanced vibrational amplitudes at the surface, which are consistent with dynamic disorder and a large accommodation coefficient at the surface. [S0031-9007(98)05625-7]

PACS numbers: 68.35.Bs, 34.50.Dy, 68.35.Ja, 92.40.Sn

The concept of a melted layer at the ice surface at temperatures -15 °C [1] has been used in the past to explain the unique properties of ice. Recently there has been considerable interest in the ability of molecules in the stratosphere to stick on the ice surface where they may react [2]. Despite a great deal of effort [3], the physical properties of the ice surface are, however, not well understood and are the subject of intensive study [4,5].

The observation of an electron diffraction pattern with peaks rotated by 30° from the expected positions lead Materer *et al.* [4,5] to suggest that the uppermost molecules vibrate so strongly that they could not be detected. In support of this suggestion, they performed molecular dynamics simulations (MDS) which, indeed, showed a substantial vibrational motion for which, so far, there is no experimental evidence. In this Letter we report the first experimental studies of the structure and phonons of the uppermost ice layer using helium atom scattering (HAS). This provides a great deal of new information on the properties of the ice surface, which allows a much better understanding of how ice interacts with its environment. Compared to electrons, neutrons, and x rays, helium atoms have the advantage that they are completely nondestructive and that they scatter exclusively from the uppermost layer without penetrating into the crystal bulk [6].

The high resolution time-of-flight (TOF) HAS apparatus used in the present measurements is similar to those described previously [6]. Nearly monoenergetic helium atoms ($\Delta v/v \approx 1\%$) are scattered from an *in situ* grown crystal mounted on a six axis sample manipulator into the detector at a total fixed scattering angle $\theta_{SD} = 95.8^\circ$. Parallel momentum transfer (ΔK_x , ΔK_y) in the surface plane can be accessed by rotating the sample polar angle ($\Delta\theta$) as well as the tilt angle (ϕ) according to

$$\Delta K_x = -2k_i \sin(\Delta\theta) \cos(\theta_{SD}/2), \quad (1)$$

$$\Delta K_y = k_i \sin(\phi) [\cos(\theta_{SD}/2 - \Delta\theta) + \cos(\theta_{SD}/2 + \Delta\theta)], \quad (2)$$

for elastic scattering. TOF spectra measured for different scattering angles reveal distinct energy gains and losses ($\pm \Delta E$) at different momentum transfers, which are then used to construct the dispersion curves of the surface phonons.

Thick ice films were grown by dosing ultrapure H_2O and D_2O [7] at a partial pressure in the range $P_{water} = 10^{-9} - 10^{-7}$ mbar onto the Pt(111) at a temperature $T_s = 125$ K. The 3D ice layer was found to be stable at $T_s \leq 125$ K for water partial pressures of about 5×10^{-11} mbar, in good agreement with previous results of Brown and George [8]. The best quality films took several hours for growth since higher adsorption rates, and lower sample temperatures, e.g., 30 K, resulted in increased surface disorder. The attenuation of the helium atom specular reflectivity during adsorption showed that, at $T_s = 125$ K, growth proceeds according to the Stranski-Krastanov mechanism, in which the formation of a complete ice bilayer [9] is followed by the creation of large domains of 3D ice.

The helium atom diffraction pattern from the surface of an ~ 100 Å (~ 40 ML) thick ice layer, grown at $T_s = 125$ K and then cooled to 30 K, is shown in the lower panel of Fig. 1. Only one quarter of the reciprocal lattice is shown, since the remaining diffraction peaks are equivalent due to symmetry. The three diffraction peaks have positions corresponding to diffraction from a hexagonal unit cell with reciprocal lattice vectors $|G| = 1.604$ Å $^{-1}$ (upper panel) which lie along the Pt(111) $[1\bar{1}0]$ azimuths making up a $(0.612 \times 0.612)R30^\circ$ incommensurate unit cell. The width of the diffraction peaks of $0.2^\circ - 0.3^\circ$ is the same as the angular resolution of the helium spectrometer, indicating large coherent ice surface domains in excess of 100 Å. A rather small quasielastic incoherent signal in TOF spectra (see below) clearly indicates that the scattering is from well ordered areas, and not from a "lattice gas" of surface defects. The relatively high background ($\sim 2.5 \times 10^4$ counts/sec) in the angular distribution in Fig. 1 is mostly due to multiphonon scattering and will be discussed later. The

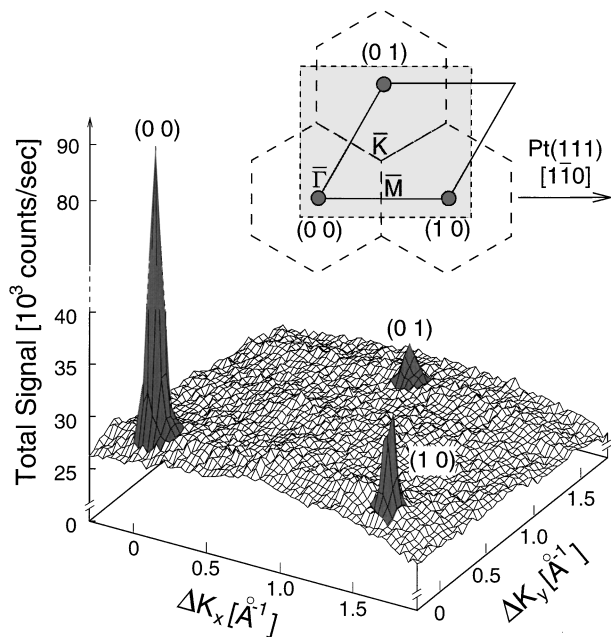


FIG. 1. A two-dimensional (2D) total signal helium diffraction pattern for a 100 Å (~ 40 ML) thick ice layer on the Pt(111) surface at an incident energy of $E_i = 22$ meV and a surface temperature of $T_s = 30$ K. Only the part of the reciprocal space between the three diffraction peaks is shown since the remaining part is equivalent due to the symmetry. The reciprocal unit cell of dimension 1.604 \AA^{-1} , as derived from the diffraction peaks, is displayed in the upper panel, which also indicates the orientation of the peaks with respect to the Pt(111) substrate and the hexagonal ice surface Brillouin zone. The shaded rectangular region shows the region of reciprocal space covered by the 2D scan.

measured ice reciprocal vectors indicate a unit cell dimension for the ice surface of $a_{\text{ice}} = 4.52 \text{ \AA}$, which is in agreement with either the (0001) surface of bulk terminated ice Ih, or the (111) surface of ice Ic [3]. The orientation of the helium diffraction peaks from the ice surface with respect to the Pt(111) surface is the same as predicted to occur for full bilayer termination of the ice crystal [3]. This is also supported by the recent LEED measurements of Materer *et al.*, which showed an unrotated ($\sim \sqrt{3} \times \sim \sqrt{3}$) diffraction pattern, and for which the upper layer of molecules was suggested to be invisible to LEED [4,5]. Thus, the present results provide the first evidence that the ice surface is terminated by a full, well ordered ice bilayer, which retains the alignment of the metal substrate template.

To complete the description of the ice surface structure it is necessary to assess the positions of the hydrogen atoms, or degree of proton order, since proton disorder has been shown to be an integral part of the bulk ice structure [10]. Using the results of a recent detailed study of the He-H₂O potential [11], the corrugation difference between an oxygen lone pair and a hydrogen atom pointing away from the surface is estimated to be $\sim 0.15 \text{ \AA}$. An

antiferroelectric ordering of the water molecules can be ruled out since if present it would lead to half-order diffraction peaks which are not observed in these experiments. Since 0.15 \AA is a substantial fraction of the He atom wavelength (1 \AA), orientational disorder would result in a large incoherent elastic signal in TOF spectra (see below). Since this is not the case for the studied ice surface we propose that the surface has predominantly either lone electron pairs or hydrogen atoms pointing away from the surface. Since the first bilayer grown on the Pt(111) surface has hydrogen atoms and not lone pairs at the surface [9], it is expected that the order of the initial bilayer is propagated to the top layer in our experiments. This observation implies that the water dipoles in the intervening layers are also ordered and, consequently, that the ice film should be at least partially ferroelectric [12].

From the temperature dependence of the specular peak, the surface Debye temperature was determined to be $\Theta_S = 175 \pm 10 \text{ K}$ which is smaller than the bulk value of $\Theta_D = 218 \pm 1 \text{ K}$ [13] as expected from the reduced coordination at the surface. The high background intensity in diffraction scans such as in Fig. 1 is known to consist of two parts, an elastic part due to incoherent scattering from surface defects [14] and an inelastic part due to scattering from single and multiphonons. Figure 2 presents several of a large series of TOF spectra for the ice surface at 30 K, measured at the same incident energy of $E_i = 22$ meV as in the diffraction scans shown in Fig. 1. The sharp peaks at $\Delta E = 0$ in Figs. 2(b)–2(d) are due to He atoms elastically scattered from symmetry breaking imperfections such as single adsorbates, boundaries between different ice domains on the surface, or proton disorder within the uppermost layer. These peaks are similar in intensity to incoherent scattering signals from “well-prepared” single crystal surfaces which are known to be highly ordered [15]. Even a very low density of surface defects ($\approx 3\%$) was shown to result in a much more intense incoherent scattering signal in TOF spectra [16]. For ice layers grown more rapidly this incoherent elastic peak was found to be significantly higher, suggesting that built-in defects, such as proton disorder or domain boundaries, are more likely.

The most interesting features of the inelastic part of the spectrum are the peaks at $\Delta E = \hbar\omega = \pm 5.9 \text{ meV}$ seen in Fig. 2. Because of the presence of both energy gain and loss peaks and the invariance of the peak position with helium beam energy and surface temperature, these peaks can be assigned to single phonon transitions on the ice surface. The momentum transfer dependence of the phonon frequencies obtained from the TOF spectra, as well as the phonon intensities, are presented in Fig. 3. Since similar sharp phonon modes were not observed for an amorphous ice layer grown at $T_s = 30 \text{ K}$, we conclude that the 5.9 meV mode arises from a collective phonon vibration and is not due to excitation of isolated molecules. This conclusion is also supported by the

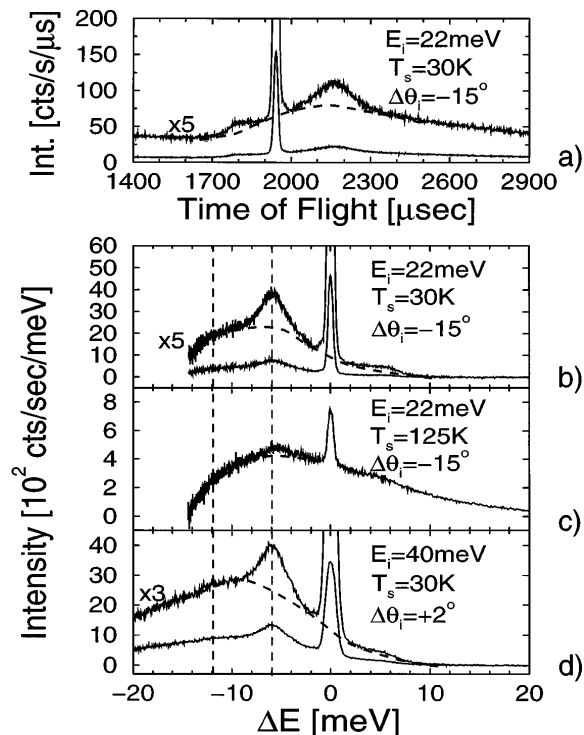


FIG. 2. Several time-of-flight spectra measured from the ice surface under different conditions in the direction of the first order ice diffraction peaks, i.e., along the Pt(111) $[1\bar{1}0]$ azimuth. (a) Shows a typical time-of-flight spectrum measured for an incident beam energy of $E_i = 22$ meV, $\Delta\theta = -15^\circ$, and a surface temperature of $T_s = 30$ K. This spectrum, when converted to energy transfer as in (b), reveals a significant diffuse elastic peak, broad phonon peaks at $\Delta E = \pm 5.9$ meV, and a broad multiphonon background (illustrated by the dashed line). The single phonon character of the -5.9 meV peak is confirmed by the lack of any frequency shift with increase in temperature to 125 K (c) and beam energy to $E_i = 40$ meV (d).

small shift in frequency of about -5% obtained upon substituting D_2O for H_2O .

The interpretation of the phonon dispersion curve in Fig. 3 is complicated by the large value of the Debye-Waller exponent for an impulsive He-surface collision [17]

$$W = [24\mu T_s(D + E_i \cos^2 \theta_i)]/k_B \Theta_s^2, \quad (3)$$

where μ is the ratio of the He atom mass to that of a surface molecule ($\mu = 0.22$) and D is the effective surface well depth ($D = 2$ meV [11]). For a beam with incident energy $E_i = 22$ meV at $T_s = 30$ K, $W \approx 1$, and, at $T_s = 125$ K, $W \approx 4$. In the simple forced oscillator model [18] the n -phonon intensity is $e^{-2W}(2W)^n/n!$ and for $W = 1$ the relative probabilities for elastic, one-phonon, and multiphonon excitation are 0.14, 0.27, and 0.59, while for $W = 4$ they are 0.0003, 0.0027, and 0.997, respectively. As found previously for the Pt(111) surface [17] for similar values of W it is no longer possible to see the vertically polarized Rayleigh phonons for which Eq. (3) is expected to provide a reliable description. These estimates

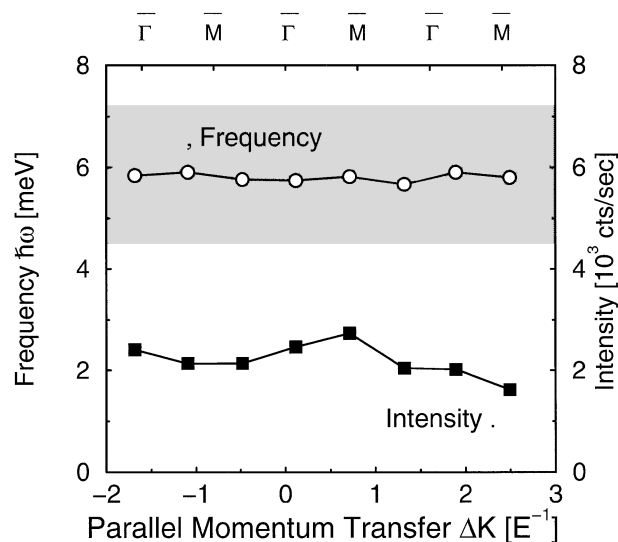


FIG. 3. Phonon frequency and inelastic peak intensity as a function of the parallel momentum transfer ΔK along the Pt $[1\bar{1}0]$ azimuth of a beam energy of 40 meV and a surface temperature of $T_s = 40$ K. The lack of a significant intensity variation is interpreted as indicating that the mode is polarized parallel to the surface. The width of the inelastic peak full width half maxima (see Fig. 2) is indicated by the gray shaded region centered at $\hbar\omega = 5.9$ meV.

are consistent with the broad multiphonon background indicated by the dashed line in the energy loss distributions in Figs. 2(b)–2(d) and with the changes in the relative intensities of the various features with incident beam energy and surface temperature. It should be pointed out here that this multiphonon background cannot be due to the Einstein-like dispersionless mode which would lead to $\pm n$ multiples of the fundamental [19].

Evidence on the polarization of the 5.9 meV surface mode comes from the weak dependence of the peak intensity on the parallel momentum transfer, ΔK , shown in Fig. 3. Dispersionless, vertically polarized modes invariably lead to a sharp peaking in their intensities at the zone origin [19], whereas dispersionless, longitudinally polarized modes exhibit only a weak dependence on ΔK [20]. Thus, the experimental evidence indicates a substantial longitudinal component of the observed 5.9 meV mode.

To check this assignment force constants previously fitted to bulk phonon dispersion curves were used to predict the expected surface phonon dispersion curves. This valence force field scheme has been found by many groups [21,22] to provide a reasonably good description of the bulk phonon dispersion curves even though long-range dipole-dipole forces are only approximately accounted for [22]. Our calculations predict, in addition to the ubiquitous Rayleigh mode, a longitudinally polarized mode at 6.7 meV with a large density of states which extends out to about one third of the Brillouin zone. It is interesting that all bulk phonon experiments [21–23] and calculations show a mode at 6.9 meV (at the Γ point) to make a

dominant contribution to the density of states. Our calculations reveal that the surface mode corresponds to a large amplitude shearing motion of adjacent bilayers in the surface region. Similar modes are observed in the layered chalcogenides, e.g., GaSe(001) [24].

Because of the fact that the observed phonon mode has no dispersion it is possible to use a single molecule approximation to estimate the vibrational amplitude at the center of the Brillouin zone. At this point the entire layer moves in unison and lateral interactions do not contribute to the vibrations. From the frequency and mass of H₂O, the vibrational amplitude is calculated to be 0.21 Å at 90 K, in agreement with the MDS value in Ref. [5]. Since this temperature corresponds to an energy of only about 8 meV anharmonic effects are expected to be small.

In summary, the special surface sensitivity of helium atom scattering and the use of lower surface temperatures has made it possible to investigate the structure and phonon dynamics of the outermost ice layer for the first time. The surface is found to exhibit an ideal full bilayer termination of the bulk ice structure, whereas the TOF measurements point to the presence of a longitudinally polarized shearing mode similar to that found in the bulk. The vibrational amplitudes determined here agree well with previous MDS values and together with strong multiphonon scattering demonstrate dynamic disorder of the ice surface. The TOF spectra indicate a substantial multiphonon contribution even at the low impact energies (22 meV) and low surface temperatures used here (30 K). According to the simple, but reliable, Baule formula [17]

$$\Delta \bar{E} = \frac{-4\mu}{(1 + \mu)^2} [E_i \cos^2 \theta_1 + D], \quad (4)$$

the energy transfer for a heavier molecule with, say, $\mu = 1$ would be a factor of 1.6 larger than observed here with He. In view of this, the efficient accommodation of molecules on the surface of ice particles in the stratosphere is not surprising [2].

We would like to thank Professor U. Buck, Professor V. Buch, Professor B. Gumhalter, and Professor J.R. Manson for very fruitful discussions, and Dr. V. Panella for providing some useful references.

[1] J.G. Dash, H. Fu, and J.S. Wettlaufer, Rep. Prog. Phys. **58**, 115 (1995).

[2] S. Solomon, Nature (London) **347**, 347 (1990); B.J. Gertner and J.T. Hynes, Science **271**, 1563 (1996).

- [3] P.A. Thiel and T.E. Madey, Surf. Sci. Rep. **7**, 211 (1987).
- [4] N. Materer, U. Starke, A. Barbieri, M.A. van Hove, G.A. Somorjai, G.J. Kroes, and C. Minot, J. Phys. Chem. **99**, 6267 (1995).
- [5] N. Materer, U. Starke, A. Barbieri, M.A. van Hove, G.A. Somorjai, G.J. Kroes, and C. Minot, Surf. Sci. **381**, 190 (1997).
- [6] J.P. Toennies, *Surface Phonons*, edited by F. de Wette, Springer Series in Surface Sciences Vol. 14 (Springer-Verlag, Heidelberg, 1988), p. 248.
- [7] The H₂O used was distilled in a Millipore ZFMQ230U4 purification unit. D₂O was supplied by Aldrich Chemical Co. Inc., Milwaukee, MN, Minimum 99.996% purity.
- [8] D.E. Brown and S.M. George, J. Phys. Chem. **100**, 4988 (1996).
- [9] A. Glebov, A.P. Graham, A. Menzel, and J.P. Toennies, J. Chem. Phys. **106**, 9382 (1997).
- [10] J.C. Li and M. Leslie, J. Phys. Chem. B **101**, 6304 (1997).
- [11] S. Green, D.J. DeFrees, and A.D. McLean, J. Chem. Phys. **94**, 1346 (1991).
- [12] S.M. Jackson and R.W. Whitworth, J. Chem. Phys. **103**, 7647 (1995).
- [13] A.J. Leadbetter, Proc. R. Soc. London A **287**, 403 (1965).
- [14] A. Glebov, J.R. Manson, J.G. Skofronick, and J.P. Toennies, Phys. Rev. Lett. **78**, 1508 (1997); C.A. Meli, E.F. Greene, G. Lange, and J.P. Toennies, Phys. Rev. Lett. **74**, 2054 (1995).
- [15] A. Glebov, W. Silvestri, J.P. Toennies, G. Benedek, and J.G. Skofronick, Phys. Rev. B **54**, 17866 (1996); G. Lange and J.P. Toennies, Phys. Rev. B **53**, 9614 (1996).
- [16] A.P. Graham, F. Hofmann, and J.P. Toennies, J. Chem. Phys. **104**, 5311 (1996).
- [17] V. Celli, D. Himes, P. Tran, J.P. Toennies, Ch. Wöll, and G. Zhang, Phys. Rev. Lett. **66**, 3160 (1991).
- [18] G. Armand and P. Zeppenfeld, Phys. Rev. B **40**, 5936 (1989).
- [19] J. Braun, D. Fuhrmann, M. Bertino, A.P. Graham, J.P. Toennies, Ch. Wöll, A. Bilić, and B. Gumhalter, J. Chem. Phys. **106**, 9922 (1997).
- [20] A.P. Graham, M.F. Bertino, F. Hofmann, and J.P. Toennies, J. Chem. Soc. Faraday Trans. **92**, 4749 (1996).
- [21] J. Li, J. Chem. Phys. **105**, 6733 (1996).
- [22] B. Renker, in *Physics and Chemistry of Ice*, edited by E. Whalley, S.J. Jones, and L.W. Gold (Toronto University Press, Toronto, 1973), p. 82.
- [23] P.T.T. Wong and E. Whalley, J. Chem. Phys. **65**, 829 (1976).
- [24] J. Skofronick and J.P. Toennies, in *Surface Properties of Layered Structures*, edited by G. Benedek (Kluwer, Dordrecht, 1992), p. 151.